



RESEARCH ARTICLE

Ablation of reactive astrocytes exacerbates disease pathology in a model of Alzheimer's disease

Loukia Katsouri  | Amy M. Birch | Alexander W. J. Renziehausen | Carolin Zach | Yahyah Aman | Hannah Steeds | Angela Bonsu | Emily O. C. Palmer | Nazanin Mirzaei | Miriam Ries | Magdalena Sastre 

Department of Brain Sciences, Imperial College London, Hammersmith Hospital, London, UK

Correspondence

Magdalena Sastre, Department of Brain Sciences, Imperial College London, Hammersmith Hospital, London W12 0NN, UK.
Email: m.sastre@imperial.ac.uk

Funding information

Alzheimer's Research Trust, Grant/Award Numbers: ART-PG2011-12, ART-PPG2009B-10; Medical Research Council; Alzheimer's Research UK, Grant/Award Numbers: PPG2009B-10, PG2011-12

Abstract

The role of astrocytes in the progression of Alzheimer's disease (AD) remains poorly understood. We assessed the consequences of ablating astrocytic proliferation in 9 months old double transgenic APP23/GFAP-TK mice. Treatment of these mice with the antiviral agent ganciclovir conditionally ablates proliferating reactive astrocytes. The loss of proliferating astrocytes resulted in significantly increased levels of monomeric amyloid- β (A β) in brain homogenates, associated with reduced enzymatic degradation and clearance mechanisms. In addition, our data revealed exacerbated memory deficits in mice lacking proliferating astrocytes concomitant with decreased levels of synaptic markers and higher expression of pro-inflammatory cytokines. Our data suggest that loss of reactive astrocytes in AD aggravates amyloid pathology and memory loss, possibly via disruption of amyloid clearance and enhanced neuroinflammation.

KEYWORDS

astrocyte, A β , glial fibrillary acidic protein (GFAP), inflammation, synapses

1 | INTRODUCTION

Neuropathological studies in patients with Alzheimer's disease (AD) and in animal models have revealed marked clustering of glial fibrillary acidic protein (GFAP)-positive astrocytes around amyloid plaques, but the eventual function and activation of astrocytes in AD still remains not well understood (Avila-Muñoz & Arias, 2014). Recently, it was shown that, in contrast to the accepted view that amyloid lesions generate chemotactic molecules that recruit astrocytes, the reactive astrocytosis associated with amyloid plaques does not appear to involve astrocytic migration (Galea et al., 2015). However, whether astrocytes proliferate or not in the AD brain is still a controversial topic (Liddel & Barres, 2017).

A beneficial role in decreasing amyloid-related pathology was postulated based on the ability of these cells to promote clearance and degradation of amyloid peptides by producing degrading proteases, including insulin degrading enzyme (IDE), neprilysin, and metalloproteases (Ries & Sastre, 2016; Yamamoto et al., 2014). In addition, astrocytes produce and secrete extracellular chaperones involved in amyloid clearance, such as Apolipoproteins E (ApoE) and J (Koistinaho et al., 2004). Most typically, astrocytes phagocytose amyloid peptides and throughout the brain of AD patients accumulate amyloid-related material of neuronal origin (Nagele, D'Andrea, Lee, Venkataraman, & Wang, 2003; Wyss-Coray et al., 2003). Furthermore, astrocytes provide trophic support to neurons (Pellerin & Magistretti, 1994), are involved in neurotransmitter uptake and recycling (Rothstein et al., 1996), and interact directly with synapses (Osborn, Kamphuis,

Loukia Katsouri and Amy M. Birch contributed equally to this study.

This is an open access article under the terms of the Creative Commons Attribution-NonCommercial-NoDerivs License, which permits use and distribution in any medium, provided the original work is properly cited, the use is non-commercial and no modifications or adaptations are made.

© 2019 The Authors. *Glia* published by Wiley Periodicals, Inc.

Wadman, & Hol, 2016), affecting synapse formation, function, and pruning (Allen & Lyons, 2018). In AD, astrocytes structurally form a protective barrier between amyloid deposits and neurons, thus helping to preserve neural tissue and restricting the negative effects of inflammation (Maragakis & Rothstein, 2006; Nicoll & Weller, 2003; Rossner, Lange-Dohna, Zeitschel, & Perez-Polo, 2005; Wyss-Coray et al., 2003). However, under certain conditions related to acute or chronic stress, astrocytes become reactive and may be deleterious. In particular, astrocytes around amyloid plaques may contribute to prolonged neuroinflammation and to nitric oxide-mediated neurotoxicity by expressing inducible-nitric oxide synthase (iNOS) (Heneka et al., 2001). This heterogeneity of astrocyte phenotypes has recently led to their classification into A1 and A2 reactive states, although in reality, these states are not so polarized (Liddel & Barres, 2017).

In vitro treatment of astrocytes with synthetic amyloid increased calcium ion-wave signaling between these cells (Bezprozvanny, 2009) and this has also been demonstrated in vivo (Kuchibhotla, Lattarulo, Hyman, & Bacskai, 2009). Increased levels of calcium may potentially enhance the release of various transmitters, such as glutamate, D-Serine, ATP, and Gamma aminobutyric acid (GABA), resulting, among others, in glutamate-mediated excitotoxicity (Lee, McGeer, & McGeer, 2011).

Studies in animal models have reported conflicting data regarding the role of astrocytes in amyloid pathology. Deletion of the genes coding for intermediate filament proteins GFAP and vimentin, which are required for astrocyte activation, resulted in significantly higher amyloid plaque load and dystrophic neurites in APP/PS1 mice (Kraft et al., 2013), although a following study with the same mouse model did not find differences on cortical area covered by plaques nor the size distribution of the deposits (Kamphuis et al., 2015). In contrast, targeting astrocytes into the hippocampus by injection of adeno-associated virus (AAV) vectors containing the astrocyte-specific Gfa2 promoter in hippocampus reduced the amyloid pathology, synaptic dysfunction, and cognitive deficits at mid-age by driving the expression of VIVIT, a peptide that interferes with the immune/inflammatory calcineurin/NFAT (nuclear factor of activated T cells) signaling pathway (Furman et al., 2012).

In light of the conflicting literature regarding the role and regulation of astrocytes in AD, we investigated changes in amyloid pathology, synaptic and neuronal density, and memory function in a mouse model of AD in which reactive proliferating astrocytes expressing GFAP are genetically ablated (Bush et al., 1999), without affecting mature GFAP-expressing astrocytes. Our data demonstrate that astrocytes contribute fundamentally to amyloid clearance and play a crucial role in memory by affecting synaptic plasticity. Combined, our data reveal that astrocytes carry out important neuroprotective functions in an AD animal model.

2 | MATERIALS AND METHODS

2.1 | Mouse models and experimental design

APP23 (Novartis) mice were used, expressing human APP751 isoform carrying the Swedish double mutation (K670N-M671L) under the control of the murine Thy1.2 expression cassette (Sturchler-Pierrat

et al., 1997). GFAP thymidine kinase (GFAP-TK) (The Jackson Laboratory) mice express the herpes simplex virus thymidine kinase (HSV-TK) targeted to astrocytes via the GFAP promoter (Bush et al., 1999). This enables selective pharmacological ablation of astrocytic proliferation. The antiviral drug ganciclovir (GCV) (Roche) is metabolized by the TK enzyme into toxic nucleoside analogues that result in the termination of DNA synthesis. All mice were of C57Bl/6 genetic background. Mice were kept in individually ventilated cages and maintained on a 12/12 hr light/dark cycle with controlled temperature and humidity, and food and water ad libitum. All in vivo testing was performed in accordance to the United Kingdom Animal (Scientific Procedures) Act (1986) and approved by Imperial College London's Animal Welfare and Ethical Review Body.

APP23 female mice were bred with GFAP-TK mice to obtain APP23/GFAP-TK double transgenic (dTg) mice ($n = 14$). At 9 months of age, dTg mice were infused into the right lateral ventricle with GCV (dTg + GCV; $n = 8$) or saline (dTg + VEH; $n = 6$) for 2 weeks using an osmotic minipump (Alzet) at a rate of $11 \mu\text{g} \cdot \mu\text{l}^{-1} \cdot \text{hr}^{-1}$. Single transgenic APP23 (APP + GCV; $n = 10$) and GFAP-TK (GFAP + GCV; $n = 9$) mice were also infused with GCV to control for the effect of the drug alone (see schematic of treatment in Figure 1a).

We chose 9 months old APP23 mice as preliminary results testing animals at 6 and 15 months of age infused subcutaneously with GCV showed too low or high astrogliosis respectively, to be able to detect changes in the levels of proliferating astrocytes by the treatment (- Figures S1 and S2). In addition, at 6 months of age the animals did not display amyloid plaques (Figure S1b) or memory loss. At 15 months of age, there were no differences in A β staining in between dTg + Veh and dTg + GCV animals (Figure S2), probably because the A β deposition at this age was massive and the loss of proliferating astrocytes might be low compared with the considerable density of resident mature astrocytes. All these observations justified the choice of 9 months old mice for the actual treatment group, when amyloid deposition and astrocyte density are detectable but not massive, animals display some amyloid plaques and start experiencing memory loss. We also tested 3–4 weeks intra-ventricular infusion of GCV, but due to high mortality and severe side effects, we decided to restrict the treatment to only 2 weeks.

On day 14–15 post-surgery, hippocampal-dependent memory was assessed using the object location task (OLT) and Y maze. Upon completion of the behavioral tests, mice were anaesthetized and transcardially perfused with ice-cold phosphate buffered saline (PBS; 0.1 M, pH 7.4). Brains were rapidly removed and the right hemisphere was immersion fixed in 4% paraformaldehyde in PBS for 48 hr, cryoprotected in 20% sucrose in PBS, and stored at 4°C for further immunohistochemical analysis. The left hemisphere was subdivided, snap-frozen in liquid nitrogen, and stored at -80°C until protein or RNA isolation.

2.2 | Behavioral tests

All behavioral testing took place in a dimly lit room without noise interference. All tests were recorded using Ethovision XT software (Noldus). An experimenter blind to the treatment groups performed

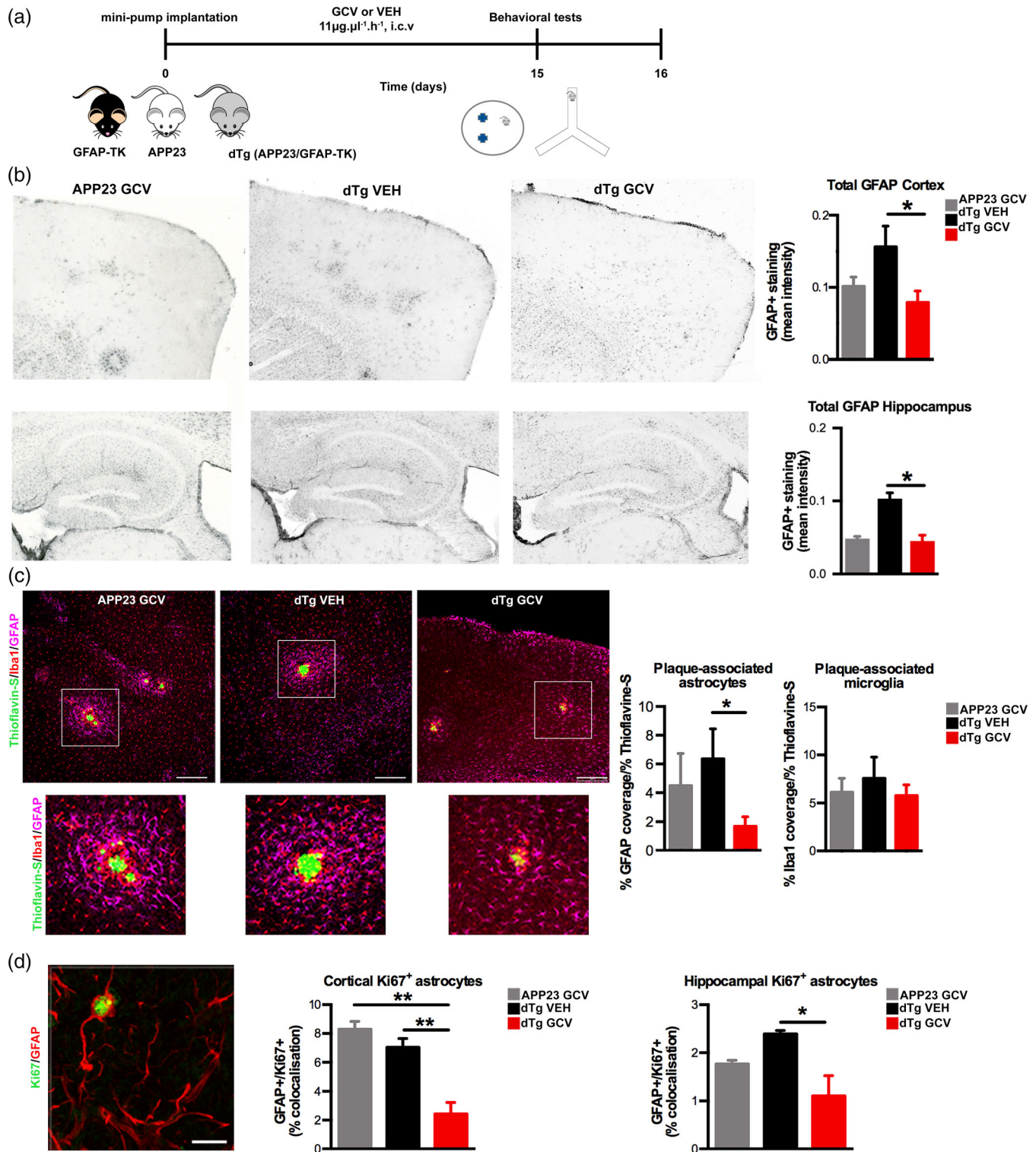


FIGURE 1 Reduction in proliferating astrocytes in dTg (APP23/GFAP-TK) mice treated with ganciclovir (GCV). (a) Schematic of the treatment. dTg mice were treated either with GCV or vehicle for 2 weeks at 9 months of age. (b) Representative images and quantification of GFAP staining in dTg mice in cortex and hippocampus; images were acquired using a 10x objective. (c) Representative images of a reduction in plaque-associated astrocytes using triple staining for Thio-S (green), GFAP (magenta), and Iba-1 (red), and quantification of area of plaque associated astrocytes (GFAP) ($n = 3-4$) and microglia (Iba-1) ($n = 3-7$) in cortex; images were acquired using a 10x objective. (d) Double staining of GFAP (red) and Ki67 (green) in the hippocampus of dTg mice treated with vehicle or GCV and quantification of the double labeled GFAP and Ki67 positive cells in cortex and hippocampus ($n = 3$); images were acquired using a 63x objective and the scale bar is 10 μm . Values shown in graphs represent the mean value \pm SEM. Statistical analysis included one-way ANOVA with Tukey's multiple-comparison post-test. * $p < .05$; ** $p < .01$. ANOVA, analysis of variance; GFAP, glial fibrillary acidic protein; Thio-S, Thioflavin-S [Color figure can be viewed at wileyonlinelibrary.com]

double-blinded scoring of all recordings from video recordings to ensure no experimental bias.

2.2.1 | Object location task

Hippocampal-dependent spatial memory was tested using the OLT, as previously reported (Katsouri et al., 2015). Mice were placed in a circular arena (diameter: 45 cm), with intramaze cues on the walls and sawdust on the floor, and allowed to freely explore for 5 min to enable habituation. Following an interval of 15–30 min, mice were returned to the arena where two identical objects made from large Lego bricks had been placed equidistant from the walls and allowed to explore for 10 min (training). Mice were then returned to their home cage and 24 hr later one of the objects was moved to a novel position within the arena. Mice were placed in the arena and allowed to explore for 5 min (testing). The total time spent actively exploring each object (sniffing or chewing) was recorded and the time spent exploring each object was calculated as a percentage of total exploration of both objects.

2.2.2 | Y maze

Spatial working memory was tested using the Y maze spontaneous alternation task. While this task is reliant on the hippocampus, other brain regions, such as the striatum, basal forebrain, and prefrontal cortex, are also involved in this task (Lalonde, Dumont, Staufenbiel, Sturchler-Pierrat, & Strazielle, 2002). Mice were placed into a single arm of the Y maze (arm length: 55 cm) and allowed to explore freely for 8 min. Extra-maze cues were present around the Y maze. The arm in which each mouse was first placed was randomized. The total number of errors were calculated by counting the number of alternate arm returns (AARs; e.g., moving from arm A to arm B then back to arm A)—2, divided by the total number of arm entries. An arm entry was counted when the mice had all four paws inside the arm.

2.3 | Total protein extraction

Brain homogenates were extracted with radioimmunoprecipitation assay buffer (1% Triton X-100, 1% sodium deoxycholate, 0.1% sodium dodecyl sulfate, 150 mM NaCl, and 50 mM Tris-HCl, pH 7.2) supplemented with Complete Protease and PhosSTOP Phosphatase inhibitor cocktails (Roche). Samples were centrifuged at 13,000 RPM for 15 min at 4°C, supernatants were collected and stored at –80°C until further analysis.

2.4 | Subcellular fractionation

Cortices were homogenized in PBS using a Dounce homogenizer, centrifuged for 45 min at 12,000 RPM at 4°C and the supernatant containing water-soluble proteins of the cytoplasm and interstitial fluid

(PBS fraction) was stored at –80°C. The pellet was resuspended in lysis buffer (PBS/Triton X-100 supplemented with protease and phosphatase inhibitors) and incubated for 20 min prior centrifugation for 10 min at 9000 RPM at 4°C. The supernatant containing all membrane-associated proteins (lysis fraction) was stored at –80°C. The remaining pellet was resuspended in Guanidine-HCl (5 M, pH 8) overnight at 4°C under constant agitation. Following centrifugation for 10 min at 9000 RPM, the supernatant containing all plaque-associated proteins (guanidine fraction) was stored at –80°C.

2.5 | Western blotting

Similar amounts of protein extracts of cortex and hippocampus were run in 4–12% NuPAGE gels (Invitrogen) followed by transfer to nitrocellulose or PVDF membranes (Katsouri et al., 2015). For A β , amyloid precursor protein (APP) and carboxyl-terminus fragments (CTFs) protein extracts in Figures S1 and S4 were immunoprecipitated with 4G8 antibody (Covance). Membranes were incubated with primary antibodies against A β (clone 6E10, Covance), postsynaptic density protein 95, PSD-95 (Abcam), synaptophysin (Millipore) and (Low density lipoprotein receptor-related protein 1) LRP-1 (kind gift from Professor Claus Pietrzik, University Mainz), IDE (Abcam) and ApoE (Santa Cruz) were used at a 1:1000 dilution, Neprilysin and glyceraldehyde 3-phosphate dehydrogenase (GAPDH) (Santa Cruz) at a 1:500 dilution, and β -actin (Abcam) at a 1:10,000 dilution. Sample loading was normalized to GAPDH or β -actin.

2.6 | Enzyme-linked immunosorbent assays

The levels of human A β 42 were determined in frontal cortex homogenates using the High Sensitivity Human Amyloid β 42 enzyme-linked immunosorbent assays (ELISA) kit from Millipore. For the mouse cytokines (Interleukin 1- β [IL-1 β], tumor necrosis factor- α [TNF α], and monocyte chemoattractant protein 1 [MCP1]) determination in cortex and hippocampus, we used kits from Peprotech. Concentrations were quantified according to the manufacturer's instructions and normalized to total protein concentration (measured by the Bradford assay).

2.7 | RNA extraction, reverse transcription, and qPCR

Tissues were lysed and homogenized in TRIzol reagent (Ambion) and total RNA was isolated using the RNeasy mini kit (Qiagen). First-strand cDNA was generated using QuantiTect Reverse Transcription kit (Qiagen) for custom-made primers. qPCR was performed using Quantifast SYBR green in a 7900HT real-time PCR system (Applied Biosystems). mRNA quantities were normalized to GAPDH (see primers in Table 1). In addition, RT2-Profiler PCR array (Qiagen) was carried out in hippocampal mRNA extracts from a dTg mouse treated with GCV compared with a dTg treated with vehicle in order to

analyze the expression of a focused panel of genes related to synaptic plasticity.

2.8 | Immunohistochemistry and immunofluorescence

Brain serial sagittal sections (40 μ m) were collected with a vibratome (Leica TV-1000S) and kept in Tris-buffered saline (TBS) pH 8.0 with 0.05% sodium azide. For A β staining, additional antigen retrieval was performed with 98% formic acid for 5 min. Sections were treated for 20 min with 0.6% H₂O₂ in TBS, permeabilized in TBS-Triton X-100 0.25% (TBS-Tx) for 30 min, and blocked for 1 hr with 10% normal horse serum (NHS) in TBS-Tx 0.1%. Sections were incubated with primary antibodies overnight at 4°C, including anti-A β antibodies MOAB-2 (6C3) (Millipore) and A β [N](IBL, Germany) at 1:1000; anti-NeuN (Millipore) at 1:500; and anti-GFAP (Invitrogen) at 1:500; anti-Iba1 (Wako) at 1:500; anti-Ki67 (Vector labs) at 1:50; synaptophysin (Santa Cruz) at 1:200 in 2% NHS in TBS-Tx 0.02%. The following day, sections were incubated with appropriate secondary antibodies (1:400; Vector), followed by enhancement with avidin-biotin complex (ABC; Vector) and 3,3'-diaminobenzidine (DAB; Sigma). Images were acquired with a Leica DM2500 microscope connected to a camera (Q-Imaging Micropublisher 3.3 RTV) using the Q-capture Pro software. For immunofluorescence, fluorescent secondary antibodies (1:400 Alexa Fluor, Invitrogen) were used. To visualize amyloid plaques, sections were incubated with 1% Thioflavin-S (Thio-S). Imaging was performed with a Zeiss LSM 780 inverted confocal microscope using ZEN software.

2.9 | Quantification of immunohistochemistry

GFAP and A β staining was quantified using ImageJ software as previously described (Katsouri et al., 2015). Briefly, the images were converted to 16-bit gray scale images, thresholded within a linear

range, and the percentage of the area covered by A β staining was calculated in the cortex and hippocampus (6–8 sections per animal, $n = 6–9$).

To quantify the GFAP- and Iba1-cells around amyloid plaques, a circular 150 μ m diameter Region of interest (ROI) was placed centered on the plaque. Within this ROI, the % coverage of ThioS staining was calculated to determine plaque size. Within the same ROI, the percentage coverage of Iba1 staining and GFAP staining were calculated. The values obtained for Iba1 (% coverage of ROI) and GFAP (%coverage of ROI) were divided by the ThioS (% coverage of the same ROI), in order to normalize the Iba1 and GFAP values to the size of the plaque (indicated by % coverage of ROI by ThioS staining). Quantification was performed around plaques in four sections per mouse ($n = 6$).

To quantify proliferating astrocytes, the number of Ki67-positive cells within clearly labeled GFAP-positive cells was calculated as a total of all Ki67-positive cells in the cortex and hippocampus.

Synaptophysin staining was quantified using ImageJ software. The images were converted to 16-bit gray scale images, thresholded within a linear range, and the percentage area coverage by the synaptophysin staining was calculated in the CA1 and CA3 (four to six sections per animal, $n = 2–4$).

For neuronal cell quantifications we measured the number of positive cells in three random squares 150 μ m \times 150 μ m for subiculum, and 100 μ m \times 100 μ m for CA3 and the area occupied by the dentate gyrus as previously described (Katsouri et al., 2015).

2.10 | Statistical analysis

All data were checked for normal distribution using the Kolmogorov-Smirnov normality test, the Levene median test to ensure that variances are equal, and the Mauchly test of sphericity before performing the appropriate statistical analysis. The data were analyzed with GraphPad Prism v6 and SPSS v20 (IBM) using two-tailed Student's *t*-test or Mann-Whitney test, one or two-way analysis of variance (ANOVA) followed by either Tukey's or Holm-Sidak's post hoc analysis. Power

TABLE 1 Primer sequences used in this study

Genes	Forward 5'-3'	Reverse 5'-3'
ApoE	GGGACAGGGGGAGTCCTATAA	ATTGGCCAGTCAGCTCCTTC
BDNF	TCATACTTCGGTTGCATGAAGG	AGACCTCTCGAACCTGCC
IDE	CAGAAGGACCTCAAGAATGGGT	GCCTCGTGGTCTCTCTTATCT
GDNF	GCCACCATTAAAAGACTGAAAAGG	GCCTGCCGATTCTCTCTCT
IL-1 β	TGCCACCTTTTGACAGTGATG	AAGGTCCACGGGAAAGACAC
iNOS	TGGTGAAGGGACTGAGCTGT	CTGAGAACAGCACAGGGGT
B-actin	CCACCATGTACCCAGGCATT	AGGGTGTAACCGCAGCTCA
TNF α	GGCTCCCTCTCATCAGTTC	CATCCCATGCCTAACTGCC
GAPDH	ACCACAGTCCATGCCATCAC	TCCACCACCCTGTTGCTGTA

Abbreviations: ApoE, Apolipoproteins E; BDNF, Brain-derived neurotrophic factor; GDNF, Glial cell-derived neurotrophic factor; IDE, insulin degrading enzyme; iNOS, inducible-nitric oxide synthase; TNF α , tumor necrosis factor- α .

Note: The table lacks the primers for NGF (Nerve growth factor) and Neprilysin: Ngf (for: 5'-CCAGTGAAATTAGGCTCCCTG-3', rev: 5'-CCTTGGCAAAACCTTTATTGGG-3'); Mme/Nep (obtained from Qiagen).

analysis was performed using GPower 3.0. All data in bar charts show means \pm SEM. Differences were considered significant for $p < .05$.

3 | RESULTS

3.1 | Effective ablation of proliferating astrocytes in APP23 mice crossed with GFAP-TK mice

To unveil the potential mechanisms by which reactive proliferating astrocytes may contribute to AD-related amyloid pathology and cognitive performance we investigated the role of proliferating astrocytes by ablating them in the APP23 mouse model of AD. We concentrated on 9 months old mice, when these animals show the first neuropathological changes of the disease and based on our pilot data (Figures S1 and S2). We crossed APP23 mice with a mouse strain that expresses HSV-TK under the control of the GFAP promoter (GFAP-TK) (Figure 1a). The resulting double transgenic mice were infused with ganciclovir (dTg + GCV) or vehicle (dTg + VEH) into the right lateral ventricle for two weeks (Figure 1a). Immunohistochemistry using GFAP as a marker of astrocytes revealed the loss of proliferating astrocytes mainly in the cortex and hippocampus of dTg + GCV compared to dTg + VEH ($p < .05$, Figures 1b and S3b), although the differences were not significant by Western blotting analysis (Figure S3a), probably because this technique detects total GFAP expression for all astrocytes, both resident mature and proliferative. In particular, we observed a significant decrease in the area covered by GFAP positive cells surrounding amyloid plaques in dTg + GCV mice compared to control dTg animals infused with saline ($p = .0379$) (dTg + VEH) (Figure 1c). Interestingly, the area of activated microglia surrounding the plaques measured by Iba-1 immunostaining showed no significant differences among groups (Figure 1c). Co-staining for GFAP and the cell proliferation marker Ki67 confirmed the significant 80% reduction in proliferating astrocytes of dTg + GCV mice in cortex ($F[2, 6] = 21.64$, $p = .0018$) and hippocampus ($F[2, 6] = 6.737$, $p = .029$) compared to control mice (Figure 1d), corroborating the efficacy of the treatment with GCV on proliferating astrocytes.

3.2 | Loss of proliferating astrocytes leads to significantly increased levels of amyloid- β

We next investigated whether ablation of proliferating reactive astrocytes affected amyloid pathology by immunohistochemistry, with monoclonal antibody 6C3. Quantification of the area covered revealed an increase in amyloid staining in the hippocampus of dTg mice treated with GCV compared to control dTg mice treated with vehicle, and to parental single transgenic APP23 mice treated with GCV ($F[2, 19] = 5.632$, $p = .012$) (Figure 2a–c). These results were confirmed by Western blotting with antibody 6E10 ($F[2, 8] = 7.361$, $p = .015$) and by ELISA for A β_{1-42} ($F[2, 8] = 8.422$, $p = .011$) in cortical brain homogenates (Figure 2d–f); however, these differences were not significant in hippocampus (Figure 2h–j), probably because there

were smaller changes in plaque associated astrocytes and GFAPKi67 positive cells in the hippocampus with the GCV treatment (Figures 1d and S3c). Similar effects were detected at 6 months of age (Figure S1c,d), but not at 15 months of age, when the density of astrocytes and amyloid deposition was considerable (Figure S2). Remarkably, we did not observe significant changes in amyloid plaque burden measured by Thio-S staining in the different groups (Figure 2a) neither on the size of the amyloid plaque (Figure S4b,c) nor in the levels of aggregated amyloid extracted upon incubation with a denaturant, guanidine hydrochloride (Figure S4a). Furthermore, differences in A β were detected at stages prior to amyloid plaque formation (Figure S1c,d), indicating that proliferating astrocyte loss particularly affected non-aggregated forms of A β . Analysis of amyloid peptide levels did not reveal any significant differences between double transgenic mice treated with vehicle and single transgenic APP23 mice treated with GCV on any of the parameters studied, as expected, indicating that the changes were not due to an effect of the GCV by itself.

To examine whether the increased amyloid peptides following reactive proliferating astrocyte ablation were due to altered amyloidogenic cleavage of APP, we evaluated the levels of total APP and the β -carboxyl terminal fragments (β -CTFs) in brain homogenates. Western blotting showed no differences in full length APP and β -CTFs in cortex (Figures 2g,k and S1d), indicating that the loss of reactive astrocytes did not affect the generation of the amyloid peptides.

Because astrocytes express proteins involved in the clearance and degradation of the amyloid peptide, we quantified the expression of lipoprotein-related mediators (ApoE and LRP1) as well as of degrading enzymes (neprilysin and IDE) in cortex (Figures 3 and S4d). dTg mice treated with GCV showed a significant reduction in the levels of ApoE mRNA ($F[2,17] = 7.51$; $p = .0046$) and protein and of neprilysin protein ($F[2,20] = 6.22$, $p = .008$) compared with dTg + VEH and APP23 + GCV mice (Figure 3). These data imply that the lack of reactive proliferating astrocytes exerted a critical role in the clearance of amyloid peptides and thereby led to increased amyloid pathology.

3.3 | Ablation of reactive astrocytes affected synaptic and neuronal density in an AD model

To investigate the eventual impact of the prevention of astrocytic proliferation on synaptic density and neurodegeneration, we measured the synaptic density by immunostaining for synaptophysin, a well-known pre-synaptic marker. Double transgenic mice treated with GCV at 9 months of age showed significant neuronal and synaptic loss in the hippocampus compared to wild-type GFAP-TK animals (Figure 4). The effect was exacerbated in particular in the CA3 area (Figure 4c). However, these changes were not detected by Western blotting of hippocampal homogenates (Figure S5a,b), suggesting that the effect was specific for a subset of neurons in the hippocampus. In addition, we observed a reduction in the number of CA3 pyramidal neurons measured by NeuN staining in dTg + GCV mice (Figure 4a,b).

After establishing defects in the hippocampal neurons, we carried out mRNA array analysis of gene expression in pathways involved in

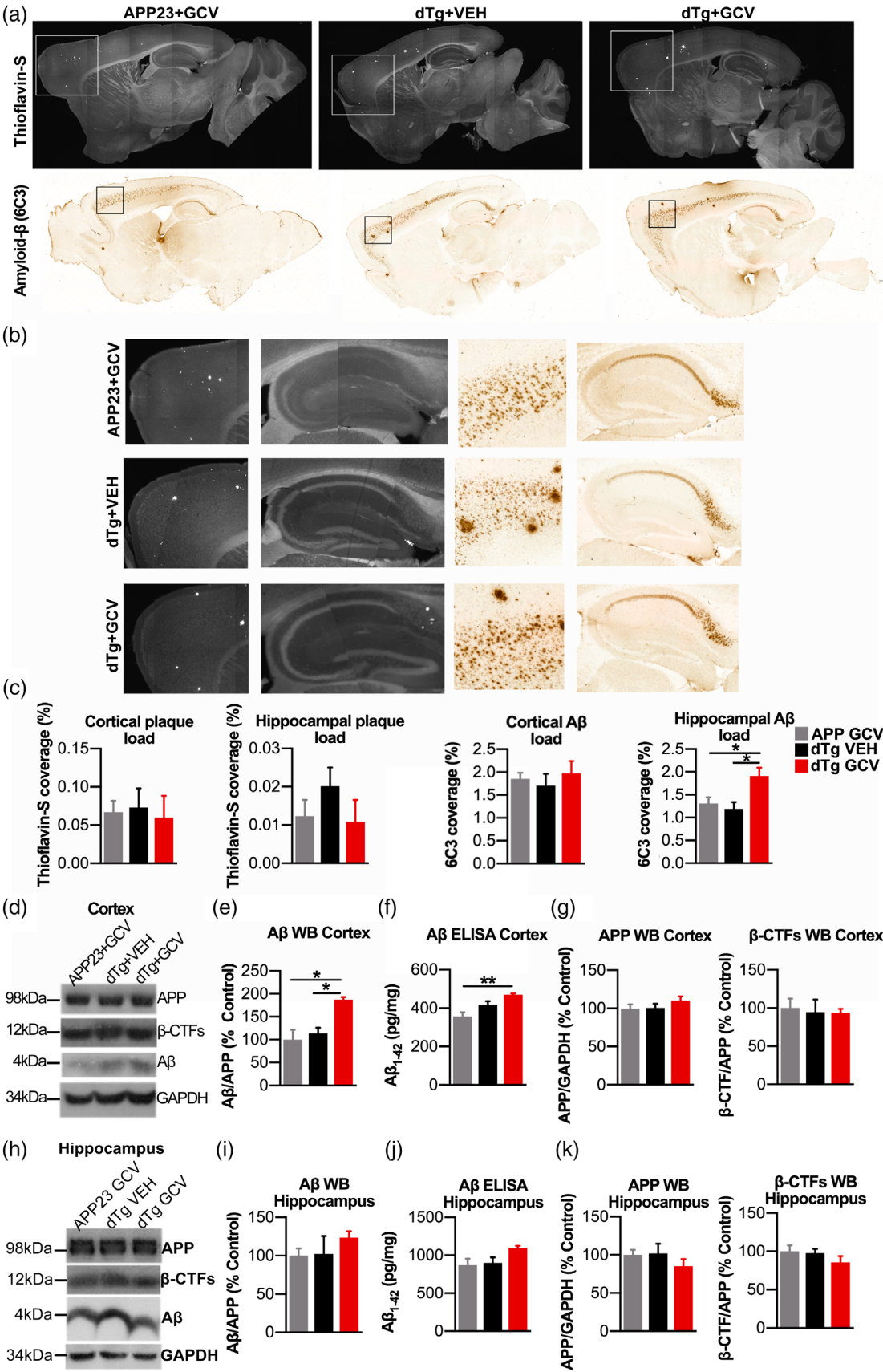


FIGURE 2 Legend on next page.

synaptic plasticity, comparing mRNA extracted from dTg mice treated with vehicle or with GCV (Figure 5a). We observed an up-regulation of genes coding for pro-inflammatory mediators including TNF α , NF κ B, nitric oxide synthase-1 (Nos1) as well as for genes coding for proteins implicated in regulation of proteases, such as tumor inhibitor of metalloproteinase1 (Timp1), the natural inhibitor of the matrix metalloproteinases in the dTg + GCV mice compared with the dTg + VEH (Figure 5a). In agreement with this, the measured levels of pro-inflammatory cytokines IL-1 β and TNF α were significantly increased in

dTg + GCV mice (Figure 5b–d). In contrast, other inflammatory mediators were reduced, including the monocyte chemoattractant protein-1 (MCP-1/CCL2) in dTg + GCV mice compared with other control groups (Figure 5b–d), as expected because these molecules are expressed by astrocytes. Various other genes that were down-regulated according to the mRNA array included neurotrophic signaling factors (Ngfr) and genes for proteins involved in neurotransmission such as GABA-A receptor- α 5 (Gabra5) and Calcineurin (Ppp3ca) as well as molecules implicated in the regulation of the fusion of

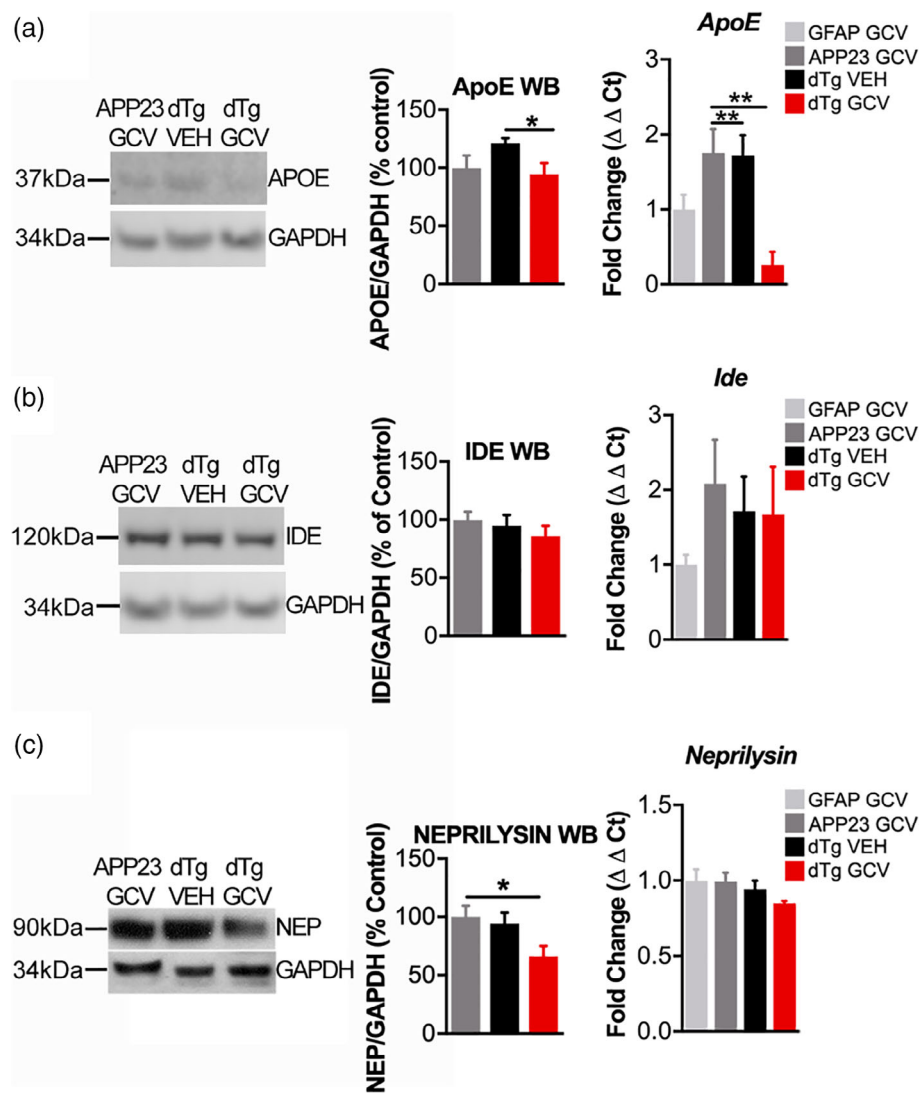


FIGURE 3 Depletion of proliferative astrocytes affects mechanisms of A β clearance. (a) Representative Western blot and quantification of ApoE protein and mRNA expression in the cortices of wild-type GFAPTK, APP23, and dTg treated with vehicle or ganciclovir (GCV) ($n = 4-8$). (b) Representative Western blot and quantification of IDE protein and mRNA expression ($n = 4-7$). (c) Representative Western blot and quantification of neprilysin protein and mRNA expression in the cortices of APP23 and dTg treated with vehicle or GCV ($n = 7-11$). Values shown in graphs represent the mean value \pm SEM. Statistical analysis included one-way ANOVA with Tukey's multiple-comparison post-test. * $p < .05$; ** $p < .01$. ANOVA, analysis of variance [Color figure can be viewed at wileyonlinelibrary.com]

FIGURE 2 Ablation of proliferating astrocytes leads to increased A β pathology in cortex. (a) Representative images of Thio-S staining (top) and 6C3 staining (bottom) in cortex and hippocampus of APP23 mice treated with ganciclovir (GCV) and dTg treated with vehicle or GCV; images were acquired using a 10 \times objective. (b) Magnification of cortex and hippocampal images of Thio-S (left) and 6C3 (right) stainings. (c) Quantification of Thio-S and 6C3 staining in cortex and hippocampus ($n = 6-9$). (d) Representative Western blotting of APP, β -CTFs, and A β with antibody 6E10 in cortex. (e) Quantification of A β by Western blot in cortex, normalized by total APP. (f) Quantification of A β 1-42 by ELISA in cortex. (g) Quantification of total APP and β -CTFs in cortex ($n = 3-4$). (h) Representative Western blots in hippocampus show no significant changes in A β load ($n = 6-11$) (i) and A β 1-42 by ELISA ($n = 4-7$) (j) and no alterations in total APP and β -CTFs (k) in dTg mice treated with GCV ($n = 7-11$). Values shown in graphs represent the mean value \pm SEM. Statistical analysis included one-way ANOVA with Tukey's multiple-comparison post-test. * $p < .05$. ANOVA, analysis of variance; APP, amyloid precursor protein; ELISA, enzyme-linked immunosorbent assays; Thio-S, Thioflavin-S [Color figure can be viewed at wileyonlinelibrary.com]

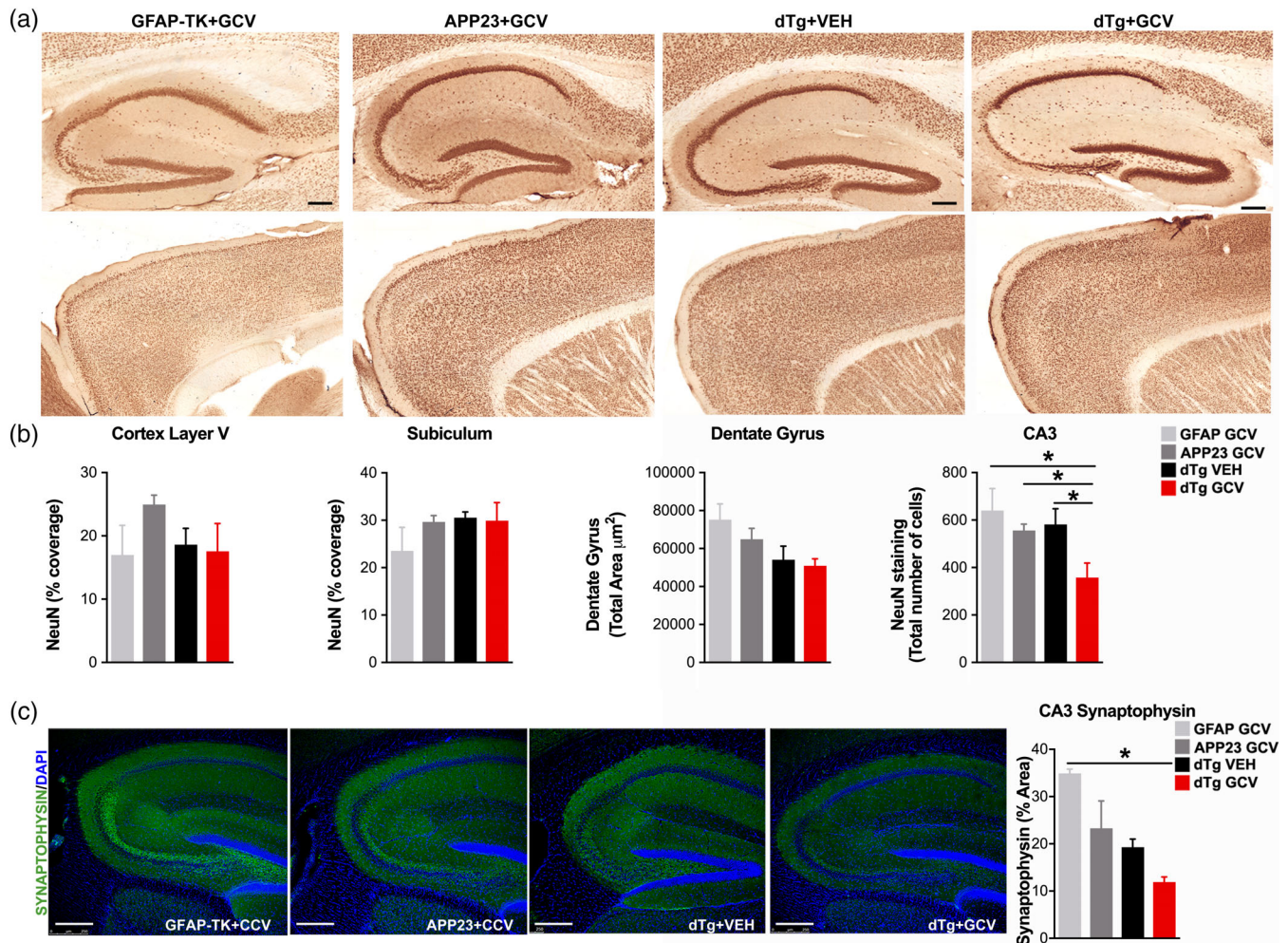


FIGURE 4 Ablation of reactive proliferating astrocytes alters neuronal and synaptic density in APP23 mice. (a) Representative images of NeuN immunoreactivity in hippocampus and cortex from GFAP-TK, APP23, and dTg treated with vehicle or ganciclovir (GCV). (b) Quantitative analysis of NeuN immunostaining in different cortical and hippocampal areas, $n = 6-8$. (c) Representative images of synaptophysin staining in the hippocampus of wild-type GFAP-TK, APP23, and dTg treated with vehicle or GCV and quantification of percentage area coverage of synaptophysin in the CA3 area of the hippocampus ($n = 3-4$). Images were acquired using a 10 \times objective values shown in graphs represent the mean value \pm SEM. Statistical analysis included one-way or two-way ANOVA with Tukey's multiple-comparison post-test. $*p < .05$. ANOVA, analysis of variance; GFAP, glial fibrillary acidic protein [Color figure can be viewed at wileyonlinelibrary.com]

synaptic vesicles (Rab3a) (Figure 5a). We confirmed the RNA array results by qPCR for several of these and other markers, however, could not find major changes in mRNA levels of growth factors, Brain-derived neurotrophic factor (BDNF), Glial cell-derived neurotrophic factor (GDNF), and Nerve Growth factor (NGF) in dTg + GCV compared with dTg + VEH mice (Figure S5c).

3.4 | Depletion of proliferating astrocytes induces hippocampal-dependent memory deficits in APP23 mice

To assess whether changes in synaptic markers and neuroinflammation were associated with alterations in hippocampal-dependent memory, mice were tested on the Y maze spatial working

memory task and the object location spatial memory task (OLT). During the OLT training, no significant differences were observed in the behavior of the mice with different genotypes and treatments (Figure 6a). However, in the subsequent OLT test all the APP23 transgenics displayed spatial memory deficits compared with GFAP-TK animals ($F[3,30] = 6.948$, $p = .001$, Figure 6b). The dTg mice were not able to discriminate between the displaced and the non-displaced object; however, dTg + GCV mice showed the lowest percentage of exploration for the displaced object (Figure 6b). Interestingly, there was a negative correlation between the performance in the OLT and the hippocampal amyloid burden, measured by 6C3 staining in all APP transgenic mice analyzed ($r = -0.47$, $p = .023$, Figure 6c). Furthermore, dTg + GCV mice showed reduced levels of spontaneous alternation and made significantly more errors, as measured by AARs, on the Y maze test ($F[3,31] = 3.19$, $p < .05$; Figure 6d). The lack of change

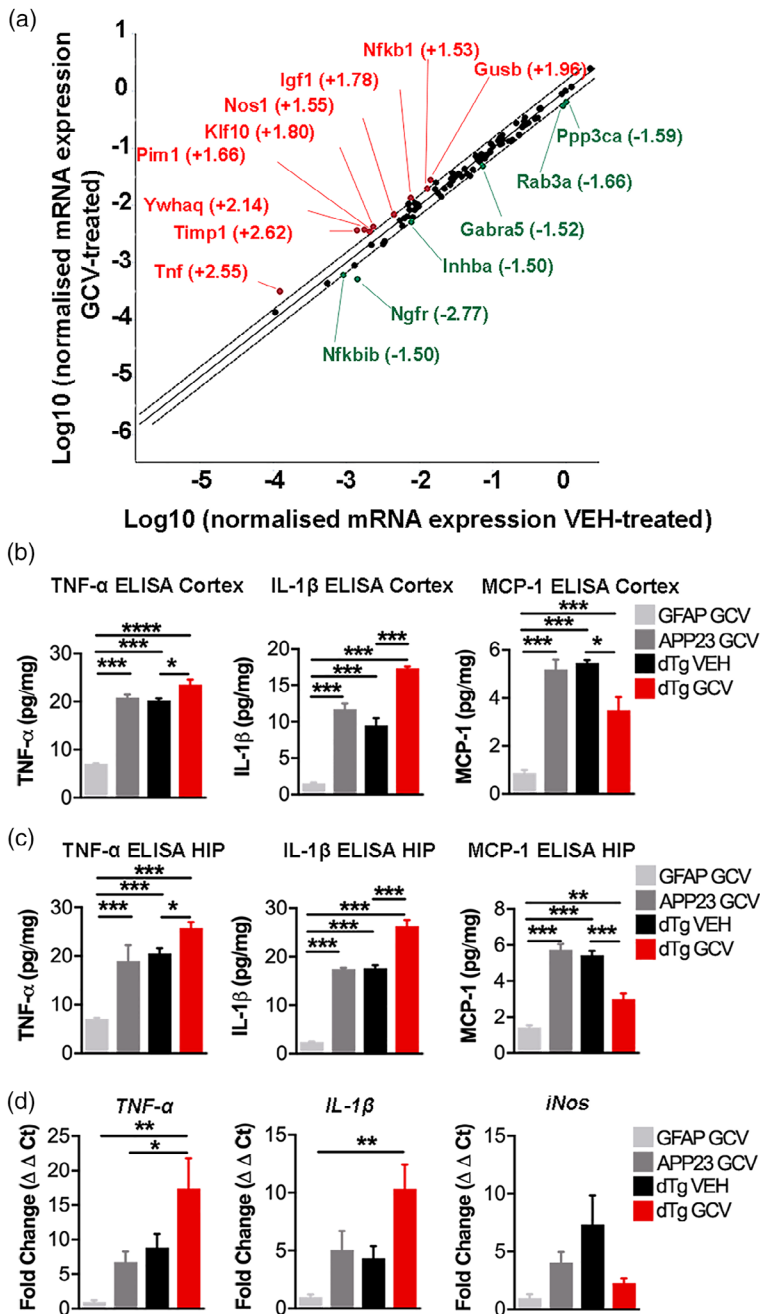


FIGURE 5 Effect of depletion of reactive astrocytes on the expression of genes involved in synaptic plasticity and neuroinflammation in hippocampus and cortex. (a) mRNA array for gene expression analysis of pathways involved in synaptic plasticity in hippocampus, comparing dTg treated with vehicle or ganciclovir (GCV). (b) Quantification of protein expression for TNF- α , IL-1 β , and MCP-1 in the cortex by ELISA (n = 4–6). (c) Quantification of protein expression for TNF- α , IL-1 β , and MCP-1 by ELISA in the hippocampus of wildtype GFAP-TK, APP23, and dTg treated with vehicle or GCV (n = 4–6). (d) Quantification of mRNA expression for Tnf- α , IL-1 β , and inducible-nitric oxide synthase (iNos) by qPCR in cortex (n = 4–8). Values shown in graphs represent the mean value \pm SEM. Statistical analysis included one-way or two-way ANOVA with Tukey's multiple comparison post-test. * p < .05; ** p < .01; *** p < .001; **** p < .0001. ANOVA, analysis of variance; ELISA, enzyme-linked immunosorbent assays; GFAP, glial fibrillary acidic protein [Color figure can be viewed at wileyonlinelibrary.com]

between the controls was not due to the GCV treatment, since no differences between another cohort of 9 months old wild-type mice and APP23 mice (both treated with vehicle) were neither detected in the Y maze test (Figure S5d). The combined data indicates that loss of reactive proliferating astrocytes leads to exacerbated pathology and memory deficits in APP23 mice.

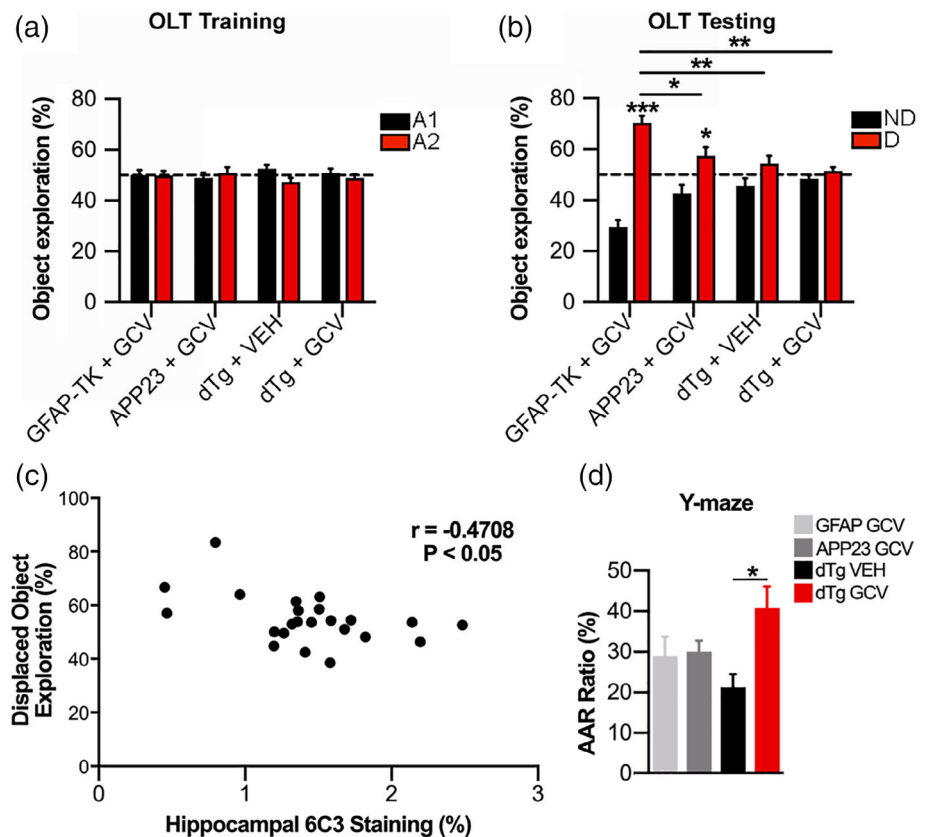
4 | DISCUSSION

The role of glial cells in the progression of AD has always been of major, if not controversial, interest invigorated by the demonstration of glial activation by amyloid peptides and by the beneficial effect of anti-

inflammatory drugs as potential add-on therapies for AD (Sastre, Klockgether, & Heneka, 2006). Contrary to previous reports regarding microglia, our findings indicate that reactive proliferating astrocytes can exert a neuroprotective effect in AD. This statement is supported by our current observations on the association of reduced proliferating astrocytes with increased amyloid pathology and synaptic loss and with reduced spatial memory in APP23 mice. A previous report by Kraft et al. (2013) using mice deficient in the astrocyte-specific proteins GFAP and vimentin crossed with APP/PS1 mice, showed increased amyloid levels and exacerbated neuritic dystrophy. In addition, and in line with our current study, no major changes in amyloid plaque load were detected in GFAP/vimentin null mice crossed with APP/PS1 mice compared with APP/PS1 control mice (Kamphuis et al., 2015).

FIGURE 6 Ablation of proliferating astrocytes induces hippocampal-dependent deficits in APP23 mice.

(a) Quantification of percentage time of exploration by object location test (OLT) during training; A1 and A2 = identical objects in training session ($n = 7-11$). (b) Quantification of percentage time of exploration by OLT during testing; ND = non-displaced and D = displaced object ($n = 7-11$). (c) Correlation between the performance in the OLT and the hippocampal amyloid burden measured by 6C3 staining in all APP transgenic mice analyzed ($r = -0.47$, $p = 0.023$, $n = 23$). (d) Percentage of alternate arm return (AAR) ($n = 6-11$). Values shown in graphs represent the mean value \pm SEM. Statistical analysis included correlation analysis, repeated measures ANOVA, or one-way ANOVA followed by Tukey's multiple-comparison post-test. $*p < .05$; $**p < .01$. ANOVA, analysis of variance; APP, amyloid precursor protein [Color figure can be viewed at wileyonlinelibrary.com]



However, both publications studied the double GFAP/vimentin knock-out mice and failed to account mechanistically for the exacerbation of AD pathology and did not measure the potential behavioral changes.

There is an ongoing debate on whether astrocytic proliferation occurs in the AD brain. Previous studies have found either no increase or a modest increase in astrocyte proliferation in animal models (Baglietto-Vargas et al., 2017; Kamphuis, Orre, Kooijman, Dahmen, & Hol, 2012) and higher numbers of GFAP(+) astrocytes in AD patients compared with non-demented controls, although both groups had similar numbers of total astrocytes double-labeled with GFAP and glutamine synthase or Aldehyde Dehydrogenase 1 Family Member (L1ALDH1L1) (Serrano-Pozo, Gómez-Isla, Growdon, Frosch, & Hyman, 2013). These outcomes may depend on the animal model used, the age, the brain area as well as the particular type of astrocyte and the marker used to identify the astrocytes. Our present observations indicate that cortex and hippocampus of APP23 mice at 9 months of age showed certain co-labeling of GFAP positive cells with Ki67, with hypertrophic morphology and mostly associated with the astrocytic scar surrounding the amyloid plaques, suggesting that their function accounts for relevant changes in amyloid deposition. In agreement with our data, ablation of proliferating astrocytes in a model of traumatic brain injury also affected the glial scar and led to neurodegeneration and increased neuroinflammation in the GFAP-TK model (Myer, Gurkoff, Lee, Hovda, & Sofroniew, 2006).

Our results indicate that reactive astrocytes are involved in the clearance of amyloid peptides, in particular monomers and small oligomers rather than plaques, which we propose to be mediated by enzymes produced by astrocytes. The contribution of ApoE to

amyloid peptide clearance was reported in young APP transgenic mice before the onset of A β deposition, showing that ApoE knock-out may increase soluble A β levels (DeMattos et al., 2004; Fagan et al., 2002). ApoE is mainly produced by astrocytes and its expression was significantly reduced in the dTg + GCV mice, as expected, which correlated with their higher amyloid peptide levels. However, ApoE is not only highly expressed in astrocytes but also in microglia (Zhao, Liu, Qiao, & Bu, 2018) and has been shown to be highly upregulated in microglia in mouse models with AD-like pathology (Keren-Shaul et al., 2017; Orre et al., 2014). Therefore, the potential influence of astrocytes on microglia function and the relative contribution of other mechanisms of amyloid clearance, such as phagocytosis and blood brain barrier and the proposed glymphatic clearance (Iliff & Nedergaard, 2013), require additional investigation in future studies.

The data-sets of comparative mRNA analysis from dTg mice treated with vehicle or GCV demonstrated alterations in the expression of genes belonging to inflammatory pathways and to neurotrophic signaling, including growth factors and cytokines produced by astrocytes. Previous studies analyzing the profile of astrocytes extracted from AD mouse brains suggest the presence of dysfunctional astrocytes in AD mouse models compared with wild-type controls, releasing increased levels of GABA (Jo et al., 2014), showing a pro-inflammatory phenotype (Orre et al., 2014) and reduced expression of genes involved in neuronal communication. A more thorough study of the potential heterogeneity of astrocytes could be accomplished by isolation of astrocytes by micro-dissection in different areas of the CNS.



An important observation of our study is the contribution of astrocytes to synaptic density in AD. APP23 mice deficient in proliferating astrocytes displayed reduced synaptophysin staining in specified areas of the hippocampus and revealed a down-regulation of genes involved in synaptic plasticity. These findings complement studies in mice deficient in astrocyte-derived synaptogenic molecules, which show reduced synapse numbers (Christopherson et al., 2005; Kucukdereli et al., 2011). Besides releasing synaptogenic molecules and neurotransmitters, astrocytes also appear to actively engulf synapses, mediating synapse pruning during development (Chung et al., 2013; Chung, Welsh, Barres, & Stevens, 2015) and clearing dysfunctional synapses or synaptic debris in disease (Gomez-Arboledas et al., 2018). Therefore, these combined results strengthen the hypothesis of an active role of astrocytes in memory formation.

Alternatively, the reduced synaptic plasticity and defective memory of the dTg + GCV mice could be a consequence of increased non-aggregated amyloid levels, which are widely thought to be neurotoxic and to induce the production of pro-inflammatory cytokines such as TNF α by glial cells (Sastre et al., 2006). The increased expression of TNF α and IL-1 β observed after ablation of proliferating astrocytes was not associated with changes in the density of microglia assessed by Iba-1 staining in the dTg + GCV mice. However, it is possible that microglia phenotype could be influenced by the interaction and the molecules released by astrocytes, as there is evidence of cross-talk between both cell types (Jha, Jo, Kim, & Suk, 2019) or instead, higher A β levels found in dTg + GCV mice could induce the activation of microglia toward a more pro-inflammatory state, without changing their number. Higher doses of GCV could potentially inhibit microglial proliferation, as suggested in mice with experimental autoimmune encephalomyelitis (EAE), a model of multiple sclerosis (Ding et al., 2014). Of note, the dose of GCV used in our study was much lower than the one in that report and was also administered to single transgenic APP23 mice, which were used as an extra control for the dTg + CGV mice.

In conclusion, our data demonstrate that proliferative astrocytes are protective in an AD model, by affecting the degradation of amyloid and reducing neuroinflammation, but their function might be different depending on the age and the disease stage, as their phenotype can change. In addition, astrocytes are quite heterogeneous in the brain, with considerable functional diversity (Ben Haim & Rowitch, 2017) and therefore different types of astrocytes could affect distinctively AD pathology. Besides investigating all these questions, future studies could explore the role of astrocytes in other relevant hallmarks of AD, such as tau pathology, since recent reports suggest that astrocytes of transgenic tau mice are functionally deficient (Sidoryk-Wegrzynowicz et al., 2017).

ACKNOWLEDGMENTS

We would like to thank Prof Claus Pietrzik (University of Mainz) for anti-LRP1 antibody, Dr Matthias Staufenbiel and Novartis for the APP23 line and Prof Fred Van Leuven (University of Leuven), and Prof Steve Gentleman (Imperial College London) for critical reading of the manuscript. This work was funded by the Alzheimer's Research UK Major Project Grant (ART-PG2011-12) and Pilot grant (ART-

PPG2009B-10) to M. S. Also, N. M. PhD studentship was funded by the Edmond J. Safra Foundation and M. R. studentship was sponsored by Imperial College Medical Research Council (MRC) Doctoral Training Centre.

CONFLICT OF INTERESTS

The authors declare no financial and non-financial competing interests.

DATA AVAILABILITY STATEMENT

The data that support the findings of this study are available on request from the corresponding author. The data are not publicly available due to privacy or ethical restrictions.

ORCID

Loukia Katsouri <https://orcid.org/0000-0003-0186-6116>

Magdalena Sastre <https://orcid.org/0000-0001-8931-6316>

REFERENCES

- Allen, N. J., & Lyons, D. A. (2018). Glia as architects of central nervous system formation and function. *Science*, 362, 181–185. <https://doi.org/10.1126/science.aat0473>
- Avila-Muñoz, E., & Arias, C. (2014). When astrocytes become harmful: Functional and inflammatory responses that contribute to Alzheimer's disease. *Ageing Research Reviews*, 18, 29–40. <https://doi.org/10.1016/j.arr.2014.07.004>
- Baglietto-Vargas, D., Sánchez-Mejías, E., Navarro, V., Jimenez, S., Trujillo-Estrada, L., Gómez-Arboledas, A., ... Gutierrez, A. (2017). Dual roles of A β in proliferative processes in an amyloidogenic model of Alzheimer's disease. *Scientific Reports*, 7, 10085. <https://doi.org/10.1038/s41598-017-10353-7>
- Ben Haim, L., & Rowitch, D. H. (2017). Functional diversity of astrocytes in neural circuit regulation. *Nature Reviews. Neuroscience*, 18, 31–41. <https://doi.org/10.1038/nrn.2016.159>
- Bezprozvanny, I. (2009). Calcium signaling and neurodegenerative diseases. *Trends in Molecular Medicine*, 15, 89–100. <https://doi.org/10.1016/j.molmed.2009.01.001>
- Bush, T. G., Puvanachandra, N., Horner, C. H., Polito, A., Ostensfeld, T., Svendsen, C. N., ... Sofroniew, M. V. (1999). Leukocyte infiltration, neuronal degeneration, and neurite outgrowth after ablation of scar-forming, reactive astrocytes in adult transgenic mice. *Neuron*, 23, 297–308.
- Christopherson, K. S., Ullian, E. M., Stokes, C. C., Mallowney, C. E., Hell, J. W., Agah, A., ... Barres, B. A. (2005). Thrombospondins are astrocyte-secreted proteins that promote CNS synaptogenesis. *Cell*, 120, 421–433. <https://doi.org/10.1016/j.cell.2004.12.020>
- Chung, W. S., Welsh, C. A., Barres, B. A., & Stevens, B. (2015). Do glia drive synaptic and cognitive impairment in disease? *Nature Neuroscience*, 18, 1539–1545. <https://doi.org/10.1038/nn.4142>
- Chung, W. S., Clarke, L. E., Wang, G. X., Stafford, B. K., Sher, A., Chakraborty, C., ... Barres, B. A. (2013). Astrocytes mediate synapse elimination through MEGF10 and MERTK pathways. *Nature*, 504, 394–400. <https://doi.org/10.1038/nature12776>
- DeMattos, R. B., Cirrito, J. R., Parsadanian, M., May, P. C., O'Dell, M. A., Taylor, J. W., ... Holtzman, D. M. (2004). ApoE and clusterin cooperatively suppress Abeta levels and deposition: Evidence that ApoE regulates extracellular Abeta metabolism in vivo. *Neuron*, 41, 193–202. [https://doi.org/10.1016/s0896-6273\(03\)00850-x](https://doi.org/10.1016/s0896-6273(03)00850-x)
- Ding, Z., Mathur, V., Ho, P. P., James, M. L., Lucin, K. M., Hoehne, A., ... Wyss-Coray, T. (2014). Antiviral drug ganciclovir is a potent inhibitor

- of microglial proliferation and neuroinflammation. *The Journal of Experimental Medicine*, 211, 189–198. <https://doi.org/10.1084/jem.20120696>
- Fagan, A. M., Watson, M., Parsadanian, M., Bales, K. R., Paul, S. M., & Holtzman, D. M. (2002). Human and murine ApoE markedly alters a beta metabolism before and after plaque formation in a mouse model of Alzheimer's disease. *Neurobiology of Disease*, 9, 305–318. <https://doi.org/10.1006/nbdi.2002.0483>
- Furman, J. L., Sama, D. M., Gant, J. C., Beckett, T. L., Murphy, M. P., Bachstetter, A. D., ... Norris, C. M. (2012). Targeting astrocytes ameliorates neurologic changes in a mouse model of Alzheimer's disease. *The Journal of Neuroscience*, 32, 16129–16140. <https://doi.org/10.1523/JNEUROSCI.2323-12.2012>
- Galea, E., Morrison, W., Hudry, E., Arbel-Ornath, M., Bacskaï, B. J., Gómez-Isla, T., ... Hyman, B. T. (2015). Topological analyses in APP/PS1 mice reveal that astrocytes do not migrate to amyloid- β plaques. *Proceedings of the National Academy of Sciences of the United States of America*, 112, 15556–15561. <https://doi.org/10.1073/pnas.1516779112>
- Gomez-Arboledas, A., Davila, J. C., Sanchez-Mejias, E., Navarro, V., Nuñez-Díaz, C., Sanchez-Varo, R., ... Gutierrez, A. (2018). Phagocytic clearance of presynaptic dystrophies by reactive astrocytes in Alzheimer's disease. *Glia*, 66, 637–653. <https://doi.org/10.1002/glia.23270>
- Heneka, M. T., Wiesinger, H., Dumitrescu-Ozimek, L., Riederer, P., Feinstein, D. L., & Klockgether, T. (2001). Neuronal and glial coexpression of argininosuccinate synthetase and inducible nitric oxide synthase in Alzheimer disease. *Journal of Neuropathology and Experimental Neurology*, 60, 906–916. <https://doi.org/10.1093/jnen/60.9.906>
- Jha, M. K., Jo, M., Kim, J. H., & Suk, K. (2019). Microglia-astrocyte crosstalk: An intimate molecular conversation. *The Neuroscientist*, 25, 227–240. <https://doi.org/10.1177/1073858418783959>
- Keren-Shaul, H., Spinrad, A., Weiner, A., Matcovitch-Natan, O., Dvir-Szternfeld, R., Ulland, T. K., ... Amit, I. (2017). A unique microglia type associated with restricting development of Alzheimer's disease. *Cell*, 169, 1276–1290.e17. <https://doi.org/10.1016/j.cell.2017.05.018>
- Iliff, J. J., & Nedergaard, M. (2013). Is there a cerebral lymphatic system? *Stroke*, 44(SUPPL1), S93–S95. <https://doi.org/10.1161/STROKEAHA.112.678698>
- Jo, S., Yarishkin, O., Hwang, Y. J., Chun, Y. E., Park, M., Woo, D. H., ... Lee, C. J. (2014). GABA from reactive astrocytes impairs memory in mouse models of Alzheimer's disease. *Nature Medicine*, 20, 886–896. <https://doi.org/10.1038/nm.3639>
- Kamphuis, W., Orre, M., Kooijman, L., Dahmen, M., & Hol, E. M. (2012). Differential cell proliferation in the cortex of the APP^{swe}PS1^{ΔE9} Alzheimer's disease mouse model. *Glia*, 60, 615–629. <https://doi.org/10.1002/glia.22295>
- Kamphuis, W., Kooijman, L., Orre, M., Stassen, O., Pekny, M., & Hol, E. M. (2015). GFAP and vimentin deficiency alters gene expression in astrocytes and microglia in wild-type mice and changes the transcriptional response of reactive glia in mouse model for Alzheimer's disease. *Glia*, 63, 1036–1056. <https://doi.org/10.1002/glia.22800>
- Katsouri, L., Ashraf, A., Birch, A. M., Lee, K. K., Mirzaei, N., & Sastre, M. (2015). Systemic administration of fibroblast growth factor-2 (FGF2) reduces BACE1 expression and amyloid pathology in APP23 mice. *Neurobiology of Aging*, 36, 821–831. <https://doi.org/10.1016/j.neurobiolaging.2014.10.004>
- Koistinaho, M., Lin, S., Wu, X., Esterman, M., Koger, D., Hanson, J., ... Paul, S. M. (2004). Apolipoprotein E promotes astrocyte colocalization and degradation of deposited amyloid-beta peptides. *Nature Medicine*, 10, 719–726. <https://doi.org/10.1038/nm1058>
- Kraft, A. W., Hu, X., Yoon, H., Yan, P., Xiao, Q., Wang, Y., ... Lee, J. M. (2013). Attenuating astrocyte activation accelerates plaque pathogenesis in APP/PS1 mice. *The FASEB Journal*, 27, 187–198. <https://doi.org/10.1096/fj.12-208660>
- Kuchibhotla, K. V., Lattarulo, C. R., Hyman, B. T., & Bacskaï, B. J. (2009). Synchronous hyperactivity and intercellular calcium waves in astrocytes in Alzheimer mice. *Science*, 323, 1211–1215. <https://doi.org/10.1126/science.1169096>
- Kucukdereli, H., Allen, N. J., Lee, A. T., Feng, A., Ozlu, M. I., Conatser, L. M., ... Eroglu, C. (2011). Control of excitatory CNS synaptogenesis by astrocyte-secreted proteins Hevin and SPARC. *Proceedings of the National Academy of Sciences of the United States of America*, 108, 440–449. <https://doi.org/10.1073/pnas.1104977108>
- Lalonde, R., Dumont, M., Staufenbiel, M., Sturchler-Pierrat, C., & Strazielle, C. (2002). Spatial learning, exploration, anxiety, and motor coordination in female APP23 transgenic mice with the Swedish mutation. *Brain Research*, 956, 36–44.
- Lee, M., McGeer, E. G., & McGeer, P. L. (2011). Mechanisms of GABA release from human astrocytes. *Glia*, 59, 1600–1611. <https://doi.org/10.1002/glia.21202>
- Liddel, S. A., & Barres, B. A. (2017). Reactive astrocytes: Production, function, and therapeutic potential. *Immunity*, 46, 957–967. <https://doi.org/10.1016/j.immuni.2017.06.006>
- Maragakis, N. J., & Rothstein, J. D. (2006). Mechanisms of disease: Astrocytes in neurodegenerative disease. *Nature Clinical Practice. Neurology*, 2, 679–689. <https://doi.org/10.1038/ncpneuro0355>
- Myer, D. J., Gurkoff, G. G., Lee, S. M., Hovda, D. A., & Sofroniew, M. V. (2006). Essential protective roles of reactive astrocytes in traumatic brain injury. *Brain*, 129, 2761–2772. <https://doi.org/10.1093/brain/awl165>
- Nagele, R. G., D'Andrea, M. R., Lee, H., Venkataraman, V., & Wang, H. Y. (2003). Astrocytes accumulate Ab42 and give rise to astrocytic amyloid plaques in Alzheimer disease brains. *Brain Research*, 971(2), 197–209.
- Nicoll, J. A., & Weller, R. O. (2003). A new role for astrocytes: Beta-amyloid homeostasis and degradation. *Trends in Molecular Medicine*, 9, 281–282.
- Orre, M., Kamphuis, W., Osborn, L. M., Jansen, A. H., Kooijman, L., Bossers, K., & Hol, E. M. (2014). Isolation of glia from Alzheimer's mice reveals inflammation and dysfunction. *Neurobiology of Aging*, 35, 2746–2760. <https://doi.org/10.1016/j.neurobiolaging.2014.06.004>
- Osborn, L. M., Kamphuis, W., Wadman, W. J., & Hol, E. M. (2016). Astroglialosis: An integral player in the pathogenesis of Alzheimer's disease. *Progress in Neurobiology*, 144, 121–141. <https://doi.org/10.1016/j.pneurobio.2016.01.001>
- Pellerin, L., & Magistretti, P. J. (1994). Glutamate uptake into astrocytes stimulates aerobic glycolysis: A mechanism coupling neuronal activity to glucose utilization. *Proceedings of the National Academy of Sciences of the United States of America*, 91, 10625–10629.
- Ries, M., & Sastre, M. (2016). Mechanisms of A β clearance and degradation by glial cells. *Frontiers in Aging Neuroscience*, 8, 160. <https://doi.org/10.3389/fnagi.2016.00160>
- Rothstein, J. D., Dykes-Hoberg, M., Pardo, C. A., Bristol, L. A., Jin, L., Kuncl, R. W., ... Welty, D. F. (1996). Knockout of glutamate transporters reveals a major role for astroglial transport in excitotoxicity and clearance of glutamate. *Neuron*, 16, 675–686.
- Rossner, S., Lange-Dohna, C., Zeitschel, U., & Perez-Polo, J. R. (2005). Alzheimer's disease beta-secretase BACE1 is not a neuron-specific enzyme. *Journal of Neurochemistry*, 92, 226–234. <https://doi.org/10.1111/j.1471-4159.2004.02857.x>
- Sastre, M., Klockgether, T., & Heneka, M. T. (2006). Contribution of inflammatory processes to Alzheimer's disease: Molecular mechanisms. *International Journal of Developmental Neuroscience*, 24, 167–176. <https://doi.org/10.1016/j.ijdevneu.2005.11.014>
- Serrano-Pozo, A., Gómez-Isla, T., Growdon, J. H., Frosch, M. P., & Hyman, B. T. (2013). A phenotypic change but not proliferation underlies glial responses in Alzheimer disease. *The American Journal of*



- Pathology*, 182, 2332–2344. <https://doi.org/10.1016/j.ajpath.2013.02.031>
- Sidoryk-Wegrzynowicz, M., Gerber, Y. N., Ries, M., Sastre, M., Tolkovsky, A. M., & Spillantini, M. G. (2017). Astrocytes in mouse models of tauopathies acquire early deficits and lose neurosupportive functions. *Acta Neuropathologica Communications*, 5, 89. <https://doi.org/10.1186/s40478-017-0478-9>
- Sturchler-Pierrat, C., Abramowski, D., Duke, M., Wiederhold, K. H., Mistl, C., Rothacher, S., ... Sommer, B. (1997). Two amyloid precursor protein transgenic mouse models with Alzheimer disease-like pathology. *Proceedings of the National Academy of Sciences of the United States of America*, 94, 13287–13292.
- Wyss-Coray, T., Loike, J. D., Brionne, T. C., Lu, E., Anankov, R., Yan, F., ... Husemann, J. (2003). Adult mouse astrocytes degrade amyloid-beta in vitro and in situ. *Nature Medicine*, 9, 453–457. <https://doi.org/10.1038/nm838>
- Yamamoto, N., Tanida, M., Ono, Y., Kasahara, R., Fujii, Y., Ohora, K., ... Sobue, K. (2014). Leptin inhibits amyloid β -protein degradation through decrease of neprilysin expression in primary cultured astrocytes. *Biochemical and Biophysical Research Communications*, 445, 214–217. <https://doi.org/10.1016/j.bbrc.2014.01.168>
- Zhao, N., Liu, C.-C., Qiao, W., & Bu, G. (2018). Apolipoprotein E, receptors, and modulation of Alzheimer's disease. *Biological Psychiatry*, 83, 347–357. <https://doi.org/10.1016/j.biopsych.2017.03.003>

SUPPORTING INFORMATION

Additional supporting information may be found online in the Supporting Information section at the end of this article.

How to cite this article: Katsouri L, Birch AM, Renziehausen AWJ, et al. Ablation of reactive astrocytes exacerbates disease pathology in a model of Alzheimer's disease. *Glia*. 2019;1–14. <https://doi.org/10.1002/glia.23759>